Mohammed A. Elmakki*, Wesley Abdul Gafoor, Orbett T. Alexander, Johan A. Venter and Andreas Roodt

The crystal structure of dicarbonyl-(*N*-nitroso-*N*-oxido-phenylamine-$\kappa^2 O,O$)-rhodium(I), $C_8H_5N_2O_4Rh$

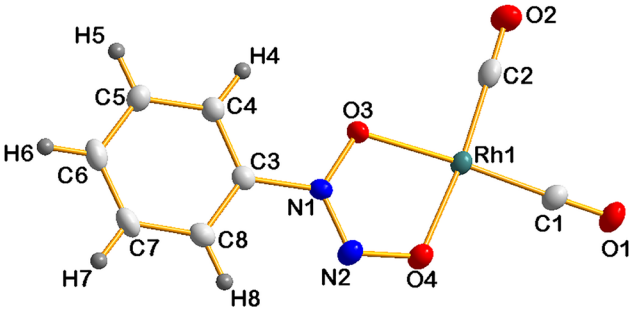

https://doi.org/10.1515/ncrs-2022-0488
Received October 5, 2022; accepted October 27, 2022; published online November 10, 2022

Abstract

$C_8H_5N_2O_4Rh$, monoclinic, $P2_1/c$ (no. 14), a = 14.1998(9) Å, b = 3.6516(2) Å, c = 17.7458(11) Å, β = 92.801(2)°, V = 919.06(10) Å^3, Z = 4, $R_{gt}(F)$ = 0.0281, $wR_{ref}(F^2)$ = 0.0702, T = 100 K.

CCDC no.: 2215630

The molecular structure is shown in the figure. Table 1 contains crystallographic data and Table 2 contains the list of the atoms including atomic coordinates and displacement parameters.

Table 1: Data collection and handling.

Crystal:	Yellow needle
Size:	0.31 × 0.06 × 0.06 mm
Wavelength:	Mo *K*α radiation (0.71073 Å)
μ:	1.85 mm^{-1}
Diffractometer, scan mode:	Bruker Apex-II, φ and ω
θ_{max}, completeness:	28.3°, >99%
$N(hkl)_{measured}$, $N(hkl)_{unique}$, R_{int}:	15,803, 2265, 0.080
Criterion for I_{obs}, $N(hkl)_{gt}$:	$I_{obs} > 2\sigma(I_{obs})$, 2073
$N(param)_{refined}$:	136
Programs:	Shelx [1], Bruker [2], Olex2 [3], Diamond [4]

Source of materials

$RhCl_3 \cdot H_2O$ (0.1000 g, 0.3798 mmol) was dissolved in 6 cm^3 DMF and refluxed for 30 min. The yellow–orange solution was cooled to room temperature. [Rh(cupf)$(CO)_2$] (cupf = *N*-nitroso-*N*-oxido-phenylamine) was synthesized by addition of *N*-nitroso-*N*-phenylhydroxylamine ammonium salt (Cupferron) (0.0589 g, 0.3798 mmol) in 3 cm^3 DMF. A yellow precipitate was formed after the addition of ice water. The precipitate was filtered off and dried. Yellow needle crystals suitable for single-crystal X-ray diffraction were obtained from hexane.

Experimental details

The aromatic H atoms were placed in geometrically idealized positions and constrained to ride on their parent atoms, with fixed C–H distances for aromatic C–H of 0.93 Å (C–H) [U_{iso} (H) = 1.2 U_{eq}]. The graphics were obtained using the Diamond [4] program with 50% probability ellipsoids. The highest peak is located 1.79 Å from C2 and the deepest hole is situated 0.78 Å from Rh1 respectively.

Comment

Oxidative addition reactions to metal complexes represent key steps in many catalytic processes, such as the carbonylation of methanol [5]. It has been shown that the oxidative addition step is the rate-determining step

***Corresponding author: Mohammed A. Elmakki**, Department of Chemistry, University of the Free State, 9301, Bloemfontein, South Africa; and Department of Chemistry, Omdurman Islamic University, 14415, Omdurman, Sudan, E-mail: azeez77777@gmail.com. https://orcid.org/0000-0002-9084-3401
Wesley Abdul Gafoor, Orbett T. Alexander, Johan A. Venter and Andreas Roodt, Department of Chemistry, University of the Free State, 9301, Bloemfontein, South Africa. https://orcid.org/0000-0003-4926-8342 (O.T. Alexander)

Table 2: Fractional atomic coordinates and isotropic or equivalent isotropic displacement parameters (Å^2).

Atom	*x*	*y*	*z*	U_{iso}*/U_{eq}
C1	0.3842 (2)	0.7990 (6)	0.71506 (16)	0.0233 (5)
C2	0.4706 (2)	0.8296 (7)	0.59281 (15)	0.0238 (5)
C3	0.17198 (16)	0.3579 (6)	0.43693 (13)	0.0177 (4)
C4	0.22717 (16)	0.3690 (6)	0.37499 (14)	0.0199 (5)
H4	0.290383	0.454419	0.379539	0.024*
C5	0.1880 (2)	0.2524 (6)	0.30607 (16)	0.0220 (5)
H5	0.224546	0.257989	0.262634	0.026*
C6	0.09543 (17)	0.1272 (6)	0.30025 (15)	0.0233 (5)
H6	0.069205	0.045391	0.252931	0.028*
C7	0.04159 (17)	0.1212 (7)	0.36266 (15)	0.0237 (5)
H7	−0.021753	0.037222	0.358049	0.028*
C8	0.07911 (19)	0.2366 (6)	0.43211 (17)	0.0213 (5)
H8	0.042304	0.232974	0.475390	0.026*
N1	0.21354 (12)	0.4765 (5)	0.50863 (10)	0.0170 (4)
N2	0.16584 (14)	0.4598 (6)	0.56735 (11)	0.0233 (4)
O1	0.40816 (14)	0.8539 (6)	0.77576 (11)	0.0326 (4)
O2	0.54526 (12)	0.9025 (6)	0.57826 (11)	0.0320 (4)
O3	0.30212 (11)	0.5986 (5)	0.50926 (9)	0.0203 (3)
O4	0.21206 (12)	0.5696 (5)	0.62922 (9)	0.0251 (4)
Rh1	0.34862 (2)	0.70847 (5)	0.61559 (2)	0.01758 (9)

in the catalytic cycles of some of these processes, and thus any effect on this step can determine the course of the complete catalytic cycle. Due to the vital role of this reaction, a significant amount of research has therefore been focused on oxidative addition reactions in order to understand its kinetic behaviour [6, 7] and responses to external and internal effects. The synthesis of Rh(I) and Rh(III) complexes have been discussed intensively, and a large number of studies comprise the synthesis of the precursor complex [Rh(*L*,*L*′-BID)$(CO)_2$], of which one of the carbonyl ligands may be substituted by tertiary phosphine ligands to form [Rh(*L*,*L*′-BID)$(CO)(PX_3)$], where *L*,*L*′-BID represents monocharged bidentate ligands with different donor atoms (*L*,*L*′) such as *O*,*O*, *O*,*N*, *O*,*S*, and *N*,*S*, with PX_3 representing different neutral monodentate tertiary phosphine ligands [5–23]. The cupferrate bidentate ligand of the title complex was selected because of its small bite angle, forming a five-membered metallocycle ring when coordinated.

In the title structure, a slightly distorted square planar geometry is observed indicated by the small bite angle of 77.879(2)° for O3–Rh1–O4, the coordinated cupferrate ligand (see the figure). The angles between the other atoms of the coordination sphere are affected as a consequence of the small bite angle and have values differing from the ideal 90°; 87.189(2)° for C1–Rh1–C2, 96.358(2)° for C2–Rh1–O3 and 98.577(2)° for C1–Rh1–O4. A crystallographic database [24] search on carbonyl bond lengths showed an average Rh–C bond length of 1.848 Å, confirming that the Rh1–C1 and Rh1–C2 bond lengths of 1.8419(1) Å and 1.8519(1) Å respectively, are in good agreement with literature values. The distance for the coordination of the two carbonyl ligands to the rhodium atom, however, differ significantly with Rh1–C2 reflecting the larger trans-influence of the nitroso oxygen (O4). The carbonyl defined by C2–O2, bound weaker than the C1–O1 carbonyl to the rhodium metal centre, is therefore the carbonyl being substituted by triphenylphosphine [9], but also forms the most stable thermodynamic isomer. The C1–O1, C2–O2, Rh1–O3 and Rh1–O4 bond lengths were determined as 1.1318(1) Å, 1.1344(1) Å, 2.0089(1) and 2.0302(1) respectively. The coordination plane (through C1, C2, O3, O4) makes (i) a dihedral angle of 16.94(4)° with the *ac*-plane, and (ii) an angle of 77.5(9)° with the weak metallophylic interaction between two successive closest Rh–Rh {distance of 3.6516(2) Å} metal centres [25]. The latter metallophylic interaction (rhodium dz^2–dz^2 orbital overlap) is much longer (weaker) than that found in a range of [RhI(*β*-diketone)$(CO)_2$] complexes (11 ligands; all forming six-membered metallocycles) which varied between 3.20 and 3.62 Å [26]. It further underlines the weak electron donating properties of the cupferrate ligand as manifested in the slow iodomethane oxidative addition observed [11].

Author contributions: All the authors have accepted responsibility for the entire content of this submitted manuscript and approved submission.

Research funding: The authors acknowledge funding under the Swiss–South Africa joint research program (SSAJRP) from the SANRF (A. Roodt: UID: 107802) as well as from the Competitive Program for Rated Researchers of the SANRF (A. Roodt: UID: 111698), from the South African Department of Science Innovation (DSI) and the Department of Science and Technology (DST) respectively, "Department of Science and Innovation, Republic of South Africa" and "Department of Science and Technology, Republic of South Africa".

Conflict of interest statement: The authors declare no conflicts of interest regarding this article.

References

1. Sheldrick G. M. A short history of *SHELX*. *Acta Crystallogr.* 2008, *A64*, 112–122.
2. Bruker. *Saint-Plus (Version 7.12) and Sadabs (Version 2004/1)*; Bruker AXS Inc.: Madison, WI, USA, 2004.
3. Dolomanov O. V., Bourhis L. J., Gildea R. J., Howard J. A. K., Puschmann H. OLEX2: a complete structure solution, refinement and analysis program. *J. Appl. Crystallogr.* 2009, *42*, 339–341.
4. Brandenburg K. *Diamond. Visual Crystal Structure Information System. 3.0c*; Crystal Impact: Bonn, Germany, 2005.

5. Maitlis P. M., Haynes A., Sunley G. J., Howard M. J. Methanol carbonylation revisited thirty years on. *J. Chem. Soc. Dalton Trans.* 1996, 2187–2196; https://doi.org/10.1039/dt9960002187.
6. Roodt A., Visser H. G., Brink A. Structure/reactivity relationships and mechanism from X-ray data and spectroscopic kinetic analysis. *Crystallogr. Rev.* 2011, *17*, 241–280.
7. Muller A. J., Otto S., Roodt A. Rapid phosphorus (III) ligand evaluation utilising potassium selenocyanate. *Dalton Trans.* 2008, 650–657; https://doi.org/10.1039/b712782k.
8. Warsink S., Kotze P. D. R., van Rensburg J. M. J., Venter J. A., Otto S., Botha E., Roodt A. Kinetic-mechanistic and solid-state study of the oxidative addition and migratory insertion of iodomethane to [rhodium(*S, O*-BdiPT or *N, O*-ox)(CO)($PR_1R_2R_3$)] complexes. *Eur. J. Inorg. Chem.* 2018, *2018*, 3615–3625.
9. Basson S. S., Leipoldt J. G., Roodt A., Venter J. A. Crystal structure of carbonyl(*N*-hydroxy-*N*-nitrosobenzenaminato-*O,O′*)-triphenylphosphinerhodium(I). *Inorg. Chim. Acta* 1986, *118*, L45–L47.
10. Elmakki M. A., Koen R., Venter J. A., Drost R. Crystal structure of dicarbonyl(pyridine-2-olate-1-oxido-κ^2*O,O′*)rhodium(I), $C_7H_4NO_4Rh$. *Z. Kristallogr. N. Cryst. Struct.* 2016, *231*, 703–705.
11. Basson S. S., Leipoldt J. G., Roodt A., Venter J. A. Mechanism for the oxidative addition of iodomethane to carbonyl(*N*-hydroxy-*N*-nitrosobenzenaminato-*O,O′*)triarylphosphinerhodium(I) complexes and crystal structure of [Rh(cupf)(CO)(CH_3)(I)(PPh_3)]. *Inorg. Chim. Acta* 1987, *128*, 31–37.
12. Uguagliati P., Deganello G., Belluco U. The system-dichlorotetracarbonyldirhodium-tertiary phosphines. *Inorg. Chim. Acta* 1974, *9*, 203–207.
13. Brink A., Roodt A., Steyl G., Visser H. G. Steric vs. electronic anomaly observed from iodomethane oxidative addition to tertiary phosphine modified rhodium(I) acetylacetonato complexes following progressive phenyl replacement by cyclohexyl [PR_3 = PPh_3, PPh_2Cy, $PPhCy_2$, PCy_3]. *Dalton Trans.* 2010, *39*, 5572–5578.
14. Elmakki M. A., Koen R., Drost R. M., Alexander O. T., Venter G. J. S., Venter J. A. Crystal structure of carbonyl (2-oxopyridin-1(2*H*-olato-κ^2*O,O′*)(triphenylphosphine-κ*P*)rhodium(I), $C_{24}H_{19}NO_3PRh$. *Z. Kristallogr. N. Cryst. Struct.* 2016, *231*, 781–783.
15. Elmakki M. A., Alexander O. T., Venter G. J. S., Venter J. A. Crystal structure of carbonyl(2-oxopyridin-1(2*H*-olato-κ^2*O,O′*) (diphenylcyclohexylphosphine-κ*P*)rhodium(I), $C_{24}H_{25}NO_3PRh$. *Z. Kristallogr. N. Cryst. Struct.* 2017, *232*, 831–833.
16. Elmakki M. A., Alexander O. T., Roodt A. The crystal structure of *trans*-carbonyl-(diphenylcyclohexyl-phosphine-κ*P*) iodidomethyl-(2-oxopyridin-1(2*H*)-olato-κ^2*O,O′*) rhodium(III), $C_{25}H_{28}INO_3PRh$. *Z. Kristallogr. N. Cryst. Struct.* 2020, *235*, 279–281.
17. Elmakki M. A., Alexander O. T., Venter J. A., Roodt A. Crystal structure of carbonyl(2-oxopyridin-1(2*H*)-olato-κ^2*O,O′*)(triphenylarsine-κ*As*) rhodium(I), $C_{24}H_{19}AsNO_3Rh$. *Z. Kristallogr. N. Cryst. Struct.* 2021, *236*, 223–225.
18. Elmakki M. A., Alexander O. T., Venter J. A., Roodt A. Crystal structure of carbonyl(2-methylquinolin-8-olato-κ^2*N,O*) (triphenylarsine-κ*As*)rhodium(I), $C_{29}H_{23}AsNO_2Rh$. *Z. Kristallogr. N. Cryst. Struct.* 2021, *236*, 215–217.
19. Elmakki M. A. E., Alexander O. T., Venter G. J. S., Venter J. A., Roodt A. Synthesis and structural determination of [Rh(opo)(CO)(PR_3)] complexes (opo^- = 2-oxopyridin-1-olate) and in situ isomeric behavior from preliminary kinetic study of iodomethane oxidative addition. *J. Coord. Chem.* 2021, *74*, 444–466.
20. Basson S. S., Leipoldt J. G., Venter J. A. Structure of pentacoordinated *b*-carbonyl-*cd*-(*N*-hydroxy-*N*-nitrosobenzenaminato-*O,O′*)-*ae*-bis(triphenylphosphine) rhodium(I). *Acta Crystallogr.* 1990, *C46*, 1324–1326.
21. Venter J. A., Leipoldt J. G., van Eldik R. Solvent, temperature, and pressure dependence of the oxidative addition of iodomethane to complexes of the type Rh^I(β-diketonate)(CO)(PPh_3). *Inorg. Chem.* 1991, *30*, 2207–2209.
22. Venter J. A., Purcell W., Visser H. G., Muller T. J. Carbonyl(*N*-nitroso-*N*-oxido-1-naphtylamine-κ^2*O,O′*) (triphenyl-phosphine-κ*P*) rhodium(I) acetone solvate. *Acta Crystallogr.* 2009, *65*, m1578–m1587.
23. Elmakki M. A., Alexander O. T., Venter J. A., Roodt A. The crystal structure of (carbonato κ^2*O, O′*)(2-oxopyridin-1(2*H*)-olato-κ*N*) tris(trimethylphosphine)rhodium(III) water solvate, $C_{15}H_{33}NO_5P_3Rh$. *Z. Kristallogr. N. Cryst. Struct.* accepted.
24. Bruno I. J., Cole J. C., Kessler M., Luo J., Motherwell W. D., Purkis L. H., Smith B. R., Taylor R., Cooper R. I., Harris S. E., Orpen A. G. Retrieval of crystallographically-derived molecular geometry information. *J. Chem. Inf. Comput. Sci.* 2004, *44*, 2133–2144.
25. Conradie M. M., Van Rooyen P. H., Pretorius C., Roodt A., Conradie J. Rhodium-rhodium interactions in [Rh(β-diketonato)$(CO)_2$] complexes. *J. Mol. Struct.* 2017, *1144*, 280–289.
26. Pretorius C. *Structural and Reactivity Study of Rhodium(I) Carbonyl Complexes as Model Nano Assemblies*. PhD thesis, University of the Free State, Bloemfontein, South Africa, 2015.